Published as: Gnanasekaran D, Shanavas A, Focke WW, Sadiku R. Polyhedral oligomeric silsesquioxane/polyamide bio-nanocomposite membranes: structure-gas transport properties. RSC Advances. 2015;5(15):11272-83.

Polyhedral oligomeric silsesquioxane/polyamide bio-nanocomposite membranes:

Structure-gas transport properties

Dhorali Gnanasekaran[a,b]*, A. Shanavas[c], Walter W Focke[a], Rotimi Sadiku[d]

[a]Institute of Applied Materials, Department of Chemical Engineering, University of Pretoria, Pretoria 0002, South Africa.
[b]Dielectric Materials Division, Central Power Research Institute, Sir C.V Raman Road, Bangalore-560 080, India
[c] Department of Chemistry, The New College (Autonomous), Chennai, India.
[d]Chemical, Metallurgical and Material Engineering, Polymer Technology Division, Tshwane University of Technology, Pretoria, South Africa

*Corresponding author. Tel.: +91 9611370795

E-mail address: gnanamster@gmail.com (Dhorali Gnanasekaran)

Abstract:

A series of bio-nanocomposite membranes based on different loadings of polyhedral oligomeric silsesquioxane (POSS) and dimer fatty acid polyamide was prepared by facile solution casting method and their gas-transport properties were evaluated using oxygen, nitrogen and carbon dioxide. Intactness of POSS molecules in the polyamide was confirmed by ^{29}Si CP/MAS NMR and FT-IR experiments. The formation of effective H-bonding interactions between POSS and polyamide was confirmed by FT-IR. The surface morphological features of the membranes prepared were analyzed using TEM, SEM and AFM techniques. TEM images revealed excellent dispersion of POSS into the membranes and it (POSS) was found to be in the range of 10 to 20 nanometers size. SEM images showed no agglomeration, even at a high content of POSS. AFM 3-D images of the membranes indicated a slight increase in surface roughness with increased POSS content. The hydrophilic/hydrophobic nature and the surface free energy of the nanocomposite membranes prepared were analysed by contact angle measurements using the Sessile drop method. Considerable influence of POSS on the glass transition temperature of the bio-nanocomposite membranes was observed. Increasing the POSS content decreased the free volume and increased the density of the membranes. These properties can be used to determine the permeability and selectivity of the membranes prepared.

Keywords: POSS; Bio-nanocomposite membranes; Gas-transport property; H-bonds

1. Introduction

Membrane science and technologies are becoming more popular and receiving more attention of researchers in the academic and industrial areas. This is due to its importance in solving some important global problems and in the development of new industrial processes that are essential for a sustainable industrial growth.[1-6] Nowadays, membrane technologies are more frequently used for the separation of wide varying mixtures in the petrochemical-related industries and thus can compete successfully with the traditional schemes.[7, 8] The main advantage of membrane gas separation is potentially an energy-saving one, because the separation process takes place without phase transition.[7] Although the currently available methods of separation operations are easy and reliable, they are expensive, energy-intensive and produce environmental pollutants. Due to the enormous potential of membranes to function as separators for mixtures of materials, there has been resurgence of interest in membrane based processes.[4] Currently, immense interests in the development of nanomaterial have opened the way for exciting new challenges and opportunities, not only in nanotechnology but in the membrane science and technologies also.[8-10]

Nanometer-sized filler materials have a large surface area-to-volume ratio, hence the volume fraction of this interfacial area is high and are of particular interest, because they can be easily dispersed in a polymer and therefore facilitating facilitate the enhancement of a desired property, such as: modulus, strength, heat resistance, barrier property and flammability.[11, 12] Therefore, polyhedral oligomeric silsesquioxane (POSS) is of particular interest, mainly, in the preparation of membranes for gas separation operations.[9, 13-24] Unlike the common nanoparticles, POSS is very small (1-3 nm) and the chemistry of POSS is quite flexible.[25] POSS molecules embody a truly hybrid inorganic core/organic shell architecture that are naturally compatible with organic hosts, such as renewable resources [26, 27] and natural biomaterials.[28, 29] In addition, it can be functionalized with various groups attached to the

apex silicon atoms, which provides good compatibility with diverse polymer matrices on a molecular level.[30, 31] In this manner, a large diversity of POSS-polymer architectures is possible.[11, 32, 33] Furthermore, POSS possesses a well-defined core and exterior surface affording a high surface area-to-volume ratio and as a porous nanofiller, their surface areas are up to 400% more than conventional microfilled composites, which is highly advantageous as this leads to property amplification.[34]

Recently, POSS with different substituents have been blended with a variety of commercial polymers.[30, 32] Besides, their relevance for practical applications, such as: barrier materials, coatings or membrane technology and gas transport operations have been well proven.[35] Instead of using an in-situ polymerization process, incorporation of POSS by employing physical blending via solution casting, has several advantages, such as: ease of processing, versatility, fast and cost-effective. The successful dispersion of POSS into polymeric matrices depends on the surface interactions of POSS via (e.g. van der Waals, strong hydrogen bonding[29]) with polymers.

Nowadays, the emphasis of the current research concentrates more on the environmental issues, waste disposal and the depletion of non-renewable resources.[36-38] Furthermore, the improved property of the renewable resources-based polymers can hasten the replacement of the petroleum-based polymers and hence, can compete or even surpass the existing petroleum-based materials on cost and performance basis and eco-friendliness.[37, 39]Accordingly, a variety of biopolymers that originate from renewable resources, such as: plant oils and agro industrial wastes; have been fabricated as bio-nanocomposites using various nanofillers. Their useful applications in therapeutic aids, medicines, heat-seal coatings printing inks, varnishes, food products and packaging materials have been realized.[26-28] Although a large number of bio-nanocomposites have been reported in the literature for various applications,[7, 26, 27, 38, 39, 40-41]to the best of our knowledge, POSS

incorporated Euramelt dimer fatty acid polyamide based bio-nanocomposite as membranes for gas transport applications have not yet been reported.

Hence, we used dimer fatty acid polyamide and incompletely condensed POSS in the preparation of bio-nanocomposite as membranes for gas transport needs for the first time. Therefore, new innovative and biosourced dimer fatty acid-based polyamides, (a special class of biopolymers, present in abundance throughout the world) are expected to be an ideal alternative chemical feedstock, since they have particularity to contain several active chemical sites (double bonds, allylic moieties, ester and amide groups) that can be used for polymerization purposes.[37]

In this context, we hereby report the morphological and gas transport properties of novel dimer fatty acid based polyhedral oligomeric silsesquioxane/polyamide (POSS/PA) bio-nanocomposite membranes, prepared by facile solution casting method. The accomplishment of effective intermolecular hydrogen bonding between the hydroxyl groups of POSS and the amide groups of dimer fatty acid, leads to the uniform dispersion of POSS particles in the membrane matrix, thereby improving the gas transport properties selectively.

2. Experimental

2.1.Materials and Methods

Heptacyclopentyl tricycloheptasiloxanetriol (POSS) was synthesized utilizing reported procedure.[42] Dimer fatty acid (Euremelt 2130) is an amorphous co-polyamide that was supplied by Huntsman. According to the supplier, this grade has a softening point in the range 138 °C to 148 °C and an amine value of ≤ 4 mg KOH/g polymer. Tetrahydrofuran (THF, Merck) was distilled using calcium hydride and sodium metal before use.

2.2.Preparation of bio-nanocomposite membranes

The POSS/PA bio-nanocomposite membranes were prepared using dimer fatty acid polyamide (Euremelt 2130) and different loadings of POSS (0, 5, 10, 15 and 20 wt.%) and

the composition of these formulations are given in Table 1. The specified amount of Euremelt 2130 was dissolved in THF at 40 °C for 48 h. Then, the calculated amount of POSS was dissolved in THF and added to Euremelt 2130 solution. Thereafter, the solution mixture was stirred for 48 h, at 40 ºC. The resulting viscous solution was transferred into a Teflon coated petridish and was kept at room temperature for 6 h in order to get the membranes. All the membranes were kept in hot air oven at 75 ºC for 24 h before use. The membrane formation capability decreased with an increasing POSS content. The bulky structure of POSS groups could have caused a decrease in the entanglement of polymer chains. The model reaction of this polymer is shown in Scheme. Membrane thickness was measured with a digital micrometer and they varied from 250 to 300 μm.

Table 1: T_g, FFV, Density and roughness of POSS/PA bio-nanocomposite membranes

Sample	POSS (g)	PA (g)	T_g (°C)	FFV	Density (g/cm^3)	R_{MAX}[a] (nm)	Rq[b] (nm)	Ra[c] (nm)
POSS-0/PA	0.0	2.0	57	0.254	1.07	-	-	-
POSS-5/PA	0.1	1.9	58	0.242	1.15	35	3.3	1.9
POSS-10/PA	0.2	1.8	59	0.230	1.22	49	5.6	4.3
POSS-15/PA	0.3	1.7	61	0.218	1.29	55	5.6	4.4
POSS-20/PA	0.4	1.6	62	0.202	1.34	82	8.0	5.6

[a] Maximum height, [b] Route mean square variation of height, [c] Average deviation of height

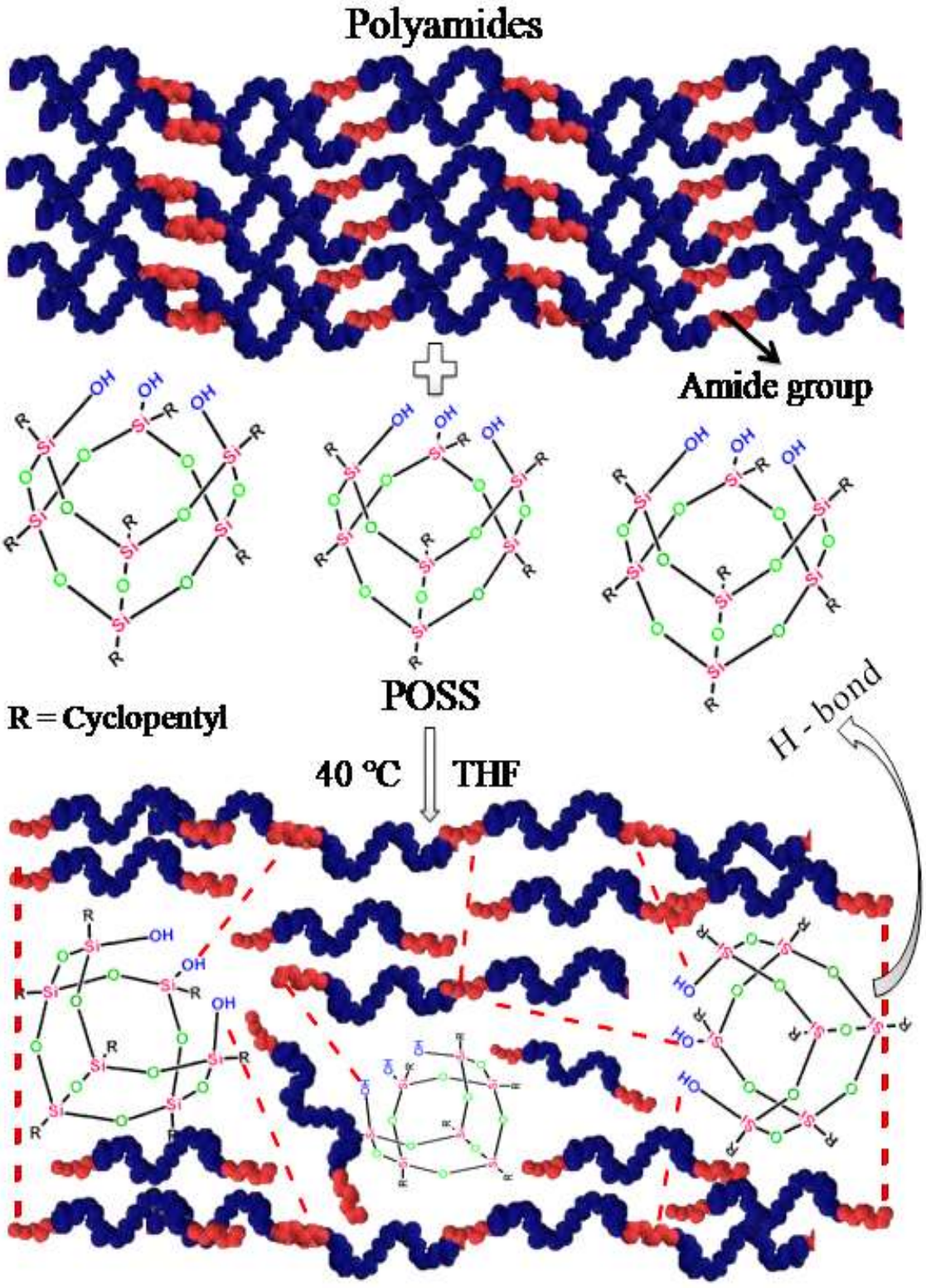

Scheme 1. Systematic methodology for preparing POSS/PA bio-nanocomposite membranes under the condition of 40 °C and in the presence of THF solvent (The possible ways of formation of H-bonds between POSS and polyamides).

2.3. Fourier transform infrared spectra

FT-IR measurements were done on Perkin-Elmer Spectrum RX 100 spectrometer in the transmission mode in order to examine the interaction between POSS particles and polyamide chains. The FT-IR spectra of these samples were recorded in the 4000–600 cm^{-1} region with 32 scans in each case, at a resolution of 4 cm^{-1}.

2.4.^{29}Si solid-state CP/MAS NMR spectroscopy

^{29}Si solid-state NMR was performed using MSL 300 MHz (Bruker) instrument to evaluate the structure of the bio-nanocomposite membranes. Cross-polarization and magic-angle spinning (CP/MAS) were used to obtain the spectra. The spinning rate was 4 kHz. A radio frequency of 62.5 kHz was used for the cross-polarization and proton decoupling (90° pulse width for ^{1}H = 4 μs). A standard Bruker 4 mm CP/MAS probe was used. Recycle delay time was 20 s.

2.5.Differential scanning calorimetry

The glass transition temperatures (T_gs) of the membranes were analysed with a Mettler-Toledo DSC 822e differential scanning calorimeter (DSC). The membranes were dried overnight under vacuum at 50 °C before the DSC measurement was done in order to eliminate adsorbed water. The analysis was performed over a temperature range of -10 to 150 °C with a heating rate of 10 °C/min and a nitrogen purge of 25 ml/min. T_g value was taken as the middle of the slope transition in the DSC curve.

2.6.Scanning Electron Microscopy

The surface morphology of the surface and cross section area of bio-nanocomposites membranes were determined using a JEOL SEM-7500F (Tokyo, Japan) equipped with EDX system, operated at an accelerating voltage of 2 kV. Thin blocks of sample were cut from the specimens and the samples were cryogenically fractured using liquid nitrogen and coating with carbon, before observing through the field emission scanning electron microscope. X-

ray spectra were recorded at 3 kV, while the electron mappings were performed at 5 kV and elements mapped include Si, C and O. Multiple images from various locations at different magnifications were collected in order to obtain an overall assessment of the POSS dispersion.

2.7.Transmission Electron Microscopy

Transmission electron microscope (TEM) (JEM-1200EX, JEOL, Tokyo, Japan) at an accelerating voltage of 100 kV was used to study the morphological structure of the bio-nanocomposits. TEM samples were prepared by dispersing bio-nanocomposites or pristine polymer in THF (1 mg/1 ml) solution on a 3 mm copper grid and dried at ambient temperature after removing excess solution, using filter paper and finally dried and used as such.

2.8.Atomic Force Microscopy

Surface morphology of the polymer composites was studied using AFM-Antonette (V. Buys) instrument Manufacturer-Bruker Model-Dimension Icon with SconAsyst and the imaging was done in tapping Mode Probe-TAP 150 at room temperature and in air. The composites were cut into small pieces and placed on a grid. The grid was covered using the commercial tip of Si_3N_4 provided by digital instruments. Cantilever length was kept at a frequency range of between 130-197 KHz spring constant of 5 N/m. The scan heads with a maximum dimension of 5 µm x 5 µm and Z scale: 100 nm. AFM images reported in this work, were reproducibly obtained over at least three points on the sample surface.

2.9.Surface energy measurements

Contact angle measurements were carried out at room temperature by Sessile drop method, using a camera mounted on a microscope to record the drop image. The surface energy of the synthesized POSS/PA nanocomposite membranes was calculated by measuring contact angle in double distilled water and hexadecane. A Digidrop (GBX) model goniometer

was used with Windrop software. An average of the results obtained from three experiments was recorded for contact angle values.

2.10. Density measurements

Density measurements, based on Archimede's Principle, of the bio-nanocomposites membrane were carried out using a Mettler AJ100 analytical balance, fitted with a Mettler ME-33360 density determination kit. The relationship between calculated density, mass and liquid density were given in the equation 1:

$$\rho_{film} = \frac{m_{air}}{m_{air} - m_{liquid}} \rho_{liquid} \quad (1)$$

Where ρ_{film} is the predicted density, m_{air} and m_{liquid} the masses measured in air and liquid, and ρ_{liquid} is the density of the liquid.

Density measurements were performed on membranes of 1cm×1cm dimensions and an average of three readings were taken for each samples. The density data of the membranes were used to estimate the chain packing by calculating the fractional free volume (FFV), from equation 2:

$$\mathrm{FFV} = \frac{\mathrm{V} - \mathrm{V_0}}{\mathrm{V}} (2)$$

Where V = total specific volume of the polymer and was obtained from the experimentally determined density of the polymer and V_o = occupied volume of the polymeric membrane. Usually, the occupied volumes are estimated to be 1.3 times more than that of Van der Waals volume, which was estimated by the Bondi[43] and Lee [44] method, by employing the group contribution correlation of Van Krevelen and Hoftyzer.[45]

2.11. Permeation measurements

Gas permeation studies of the POSS/PA bio-nanocomposite membranes were determined by using a variable pressure, constant volume ("time lag") method. The temperature was maintained at 30 ±1 °C. Gas flow rates were calculated with a soap-film bubble flow meter

apparatus. Penetrant gases were forced through in order to permeate the membrane and flow into the soap bubble flow meter, raising the bubble level. Steady state permeation i.e., (dv/dt) was achieved when soap bubble displacement was a linear function of time. The upstream pressure was varied from 1 to 4 bar (101 to 405 kPa), whereas the downstream pressure was kept at atmospheric pressure. Each measurement was repeated 3 times and for each POSS/PA composition, three membrane samples were measured. The gas permeability coefficient of pure gas, P [cm^3(STP).cm/(cm^2.s.cmHg)], was determined from equation 3:

$$P = \frac{Jd}{p_2 - p_1} = \frac{Jd}{\Delta P} \qquad (3)$$

Where J [cm^3(STP)/(cm^2.s)] is the steady state permeate flux, d is the membrane thickness (cm) and p_2 and p_1 are the feed and permeate pressures (cmHg), respectively. The steady state permeates flux, J was calculated using equation 4:

$$J = \left(\frac{dv/dt}{A}\right)\left(\frac{273.15}{T}\right)\left(\frac{P_a}{76}\right) \qquad (4)$$

Where dv/dt is the volumetric displacement rate of soap film in the soap bubble flow meter, A is the membrane area (cm^2), T is the temperature (K) and P_a is the atmospheric pressure. The selectivity ($\alpha_{A/B}$) of the bio-nanocomposite membranes for components A and B was obtained from the ratio of pure gas permeabilities.

3. Results and discussion

3.1.Structural characterizations

3.1.1. FT-IR

The FT-IR spectra of neat polyamide and POSS/PA bio-nanocomposite membranes with different loadings of POSS are shown in Fig. 1. The FT-IR results suggest that the interaction between POSS particles and amide polymer did occur through hydrogen bonding. The spectrum of neat polyamide shows its characteristic stretching frequencies of >N–H and

>C=O groups at 3355 and 1656 cm^{-1}, respectively. In the case of POSS/PA bio-nanocomposite membranes, a gradual shift to lower frequencies (from 3355 cm^{-1} to 3339 cm^{-1}) in the absorption of >N–H group of polyamide is observed and this confirms the formation of hydrogen bonding between >N–H group of polyamide and the Si-O-Si linkage of POSS. Similarly, a shift to lower frequencies in the absorption of >C=O group of polyamide reveals that the carbonyl groups are engaged in the hydrogen bonding with the hydroxyl groups of POSS. Similar phenomena have also been reported by previous researchers.[19, 46, 47] Furthermore, a new peak appeared at 1121 cm^{-1}, which is attributed to the Si-O-Si linkage of POSS and the intensity of that peak is found to have increased in the spectra of samples with higher loadings of POSS (shown in box). These features confirmed the existence of effective hydrogen bonding interactions in the POSS/PA bio-nanocomposite membranes.

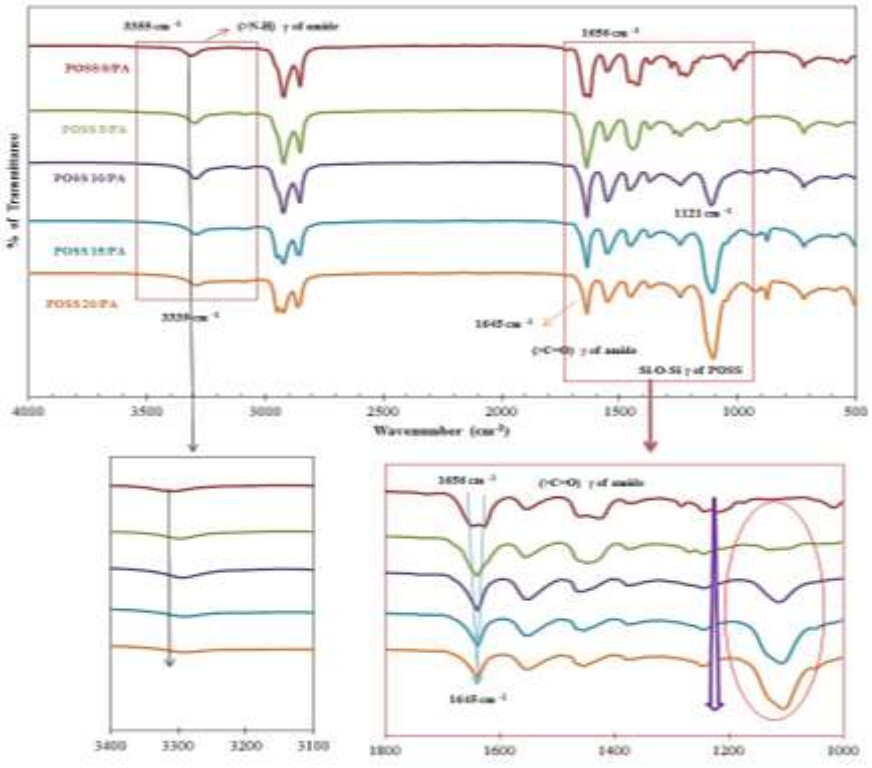

Figure 1: FT-IR spectra of POSS/PA bio-nanocomposite membranes. Intensity of H-Bonding, shifting of frequencies of >C=O and >N–H groups and the formation of new band at 1121 $cm^{-1}$for Si-O-Si linkage are highlighted in the box.

3.1.2.[29]Si Solid-state CP/MAS NMR spectroscopy

One of the membranes prepared was subjected to the solid-state [29]Si CP/MAS NMR experiment in order to confirm the binding of POSS molecules with the polymer matrix and the resulting spectrum is shown in Fig. 2. POSS molecule consists of three types of silicon atoms which are labeled as: 'a', 'b' and 'c'. Amongst these, 'a' represents the silicon atoms attached with hydroxyl groups whereas 'b' and 'c' represent the second and third silicon atoms with respect to 'a'. The spectrum in Fig. 2, shows two resonances with equal intensities at -57.29 and -66.66 ppm for the silicon atoms 'a' and 'b', respectively and a low intense signal at -65.07 ppm for silicon atom 'c'. The number of signals, intensity and chemical shift values observed in this spectrum are highly comparable and consistent with the spectrum reported [23] in the literature for POSS molecules. These observations clearly suggest that the POSS molecule has maintained its structure and remained intact during nanocomposite formation with dimer fatty acid.[48]

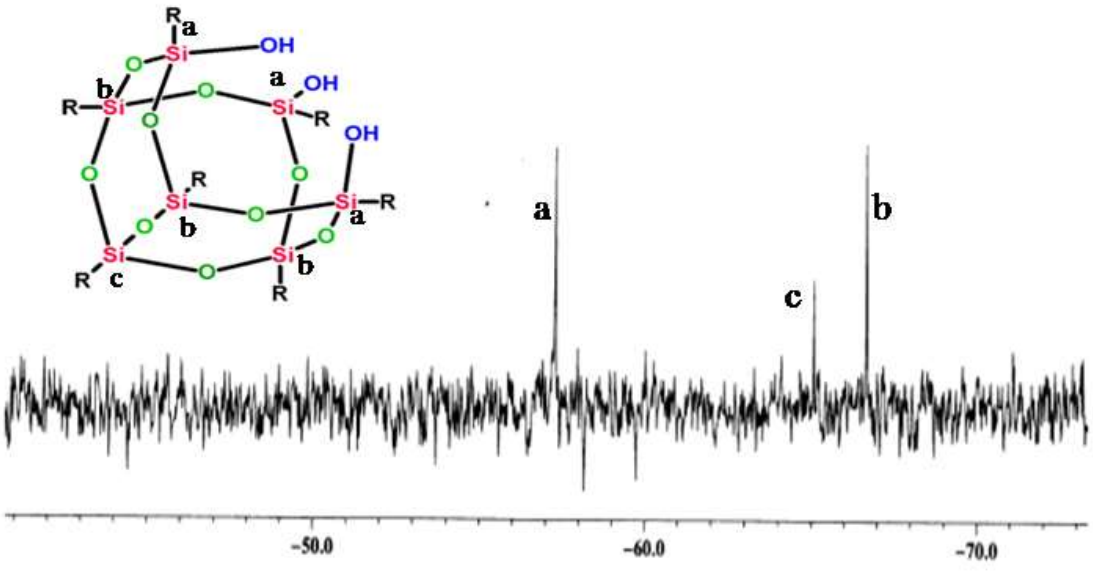

Figure 2: [29]Si CP/MAS NMR spectrum of POSS-10/PA bio-nanocomposite membrane explains the POSS molecules retain its cubic structure after membrane formation (intactness of POSS while formation of membrane).

3.2.Differential Scanning Calorimetry (DSC)

DSC experiments were carried out in order to determine the glass transition temperature (T_g) and the thermograms are shown in Fig. 3. T_g is an important index for the estimation of chain flexibility or rigidity of polymer materials. Table 1 lists the T_g values of the neat PA membrane and POSS embedded POSS/PA membranes. It is clearly evident from the Fig. 3 and Table 1 that the incorporation of POSS into PA membranes increased the T_g from 57 to 62 °C. A similar trend has been observed by Madhavan and Reddy [49] Madhavan and Reddy.[16] In addition, the T_g observed was single and suggesting that the polymers were not phase separated. The single T_g for each membrane and the variation of T_g values following POSS introduction indicate that the mixing of the POSS and PA polymer chains is at molecular level and these results are consistent with SEM and AFM. The mobility of polymer chains may be constrained by the hydrogen bonding interaction between the amide group polymer chains and the hydroxyl groups on POSS molecules, which is illustrated in the FT-IR spectra as mentioned earlier. In addition, the hydrogen bonding between POSS molecules and the PA matrix might have hindered torsional motions of the chain segments, resulting in an increase in the chain stiffness and hence the T_g, as observed. The increase in T_g for POSS incorporated membranes is due to the nano reinforcement of POSS molecule in the polymer matrices, which restricts the motions of the polymer chains. The enhancement in the T_g could have resulted from the restriction of segmental motion of molecular chains and the network junctions by the massive and bulky nanosized POSS cages. POSS leads to an increase in glass transition temperature of the PA domain and consequently the permeability of the membrane decreased or in other words, it decreased the flexibility of the polyamide blocks. Consequently the diffusion of gas also decreased substantially after the incorporation of POSS into the polyamide.

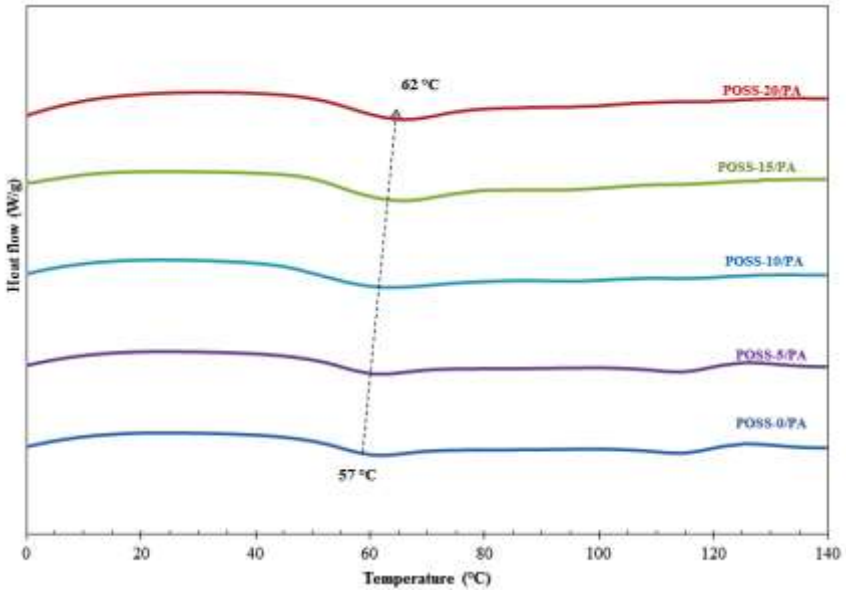

Figure 3: The DSC thermograms of POSS/PA bio-nanocomposite membranes. The Gradual increase in the glass transition temperature from 57° C to 62 °C, when increasing the POSS content, is indicated by the arrow line.

3.3.Surface morphology studies of polymeric membranes

3.3.1.Transmission electron microscopy

Transmission electron microscopy is an excellent technique to visualize the surface structure of the nanocomposites and this provides pertinent information on the dispersion behavior of the POSS in the bio-nanocomposites. Fig. 4 shows TEM micrographs of 5%, 10%, 15% and 20% POSS incorporated POSS/PA bio-nanocomposite membranes. The dark dots on the bright surface in Fig. 4 replicate the dispersion of POSS molecules on the polymer matrix. These dark dots do not stick with neighbours and tend to be separated by a constant distance from one another. This is because, during the formation of nanocomposites, POSS molecules preferentially enter into polyamide, where they undergo physical bonding between amide group of dimer fatty acid and hydroxyl group of POSS, thereby accounting for the complete disruption of the agglomerated structure at lower content of POSS (5 % and 10%). Thus, the size and distribution of POSS aggregates depend strongly on the type and strength of the intermolecular interactions.[30]

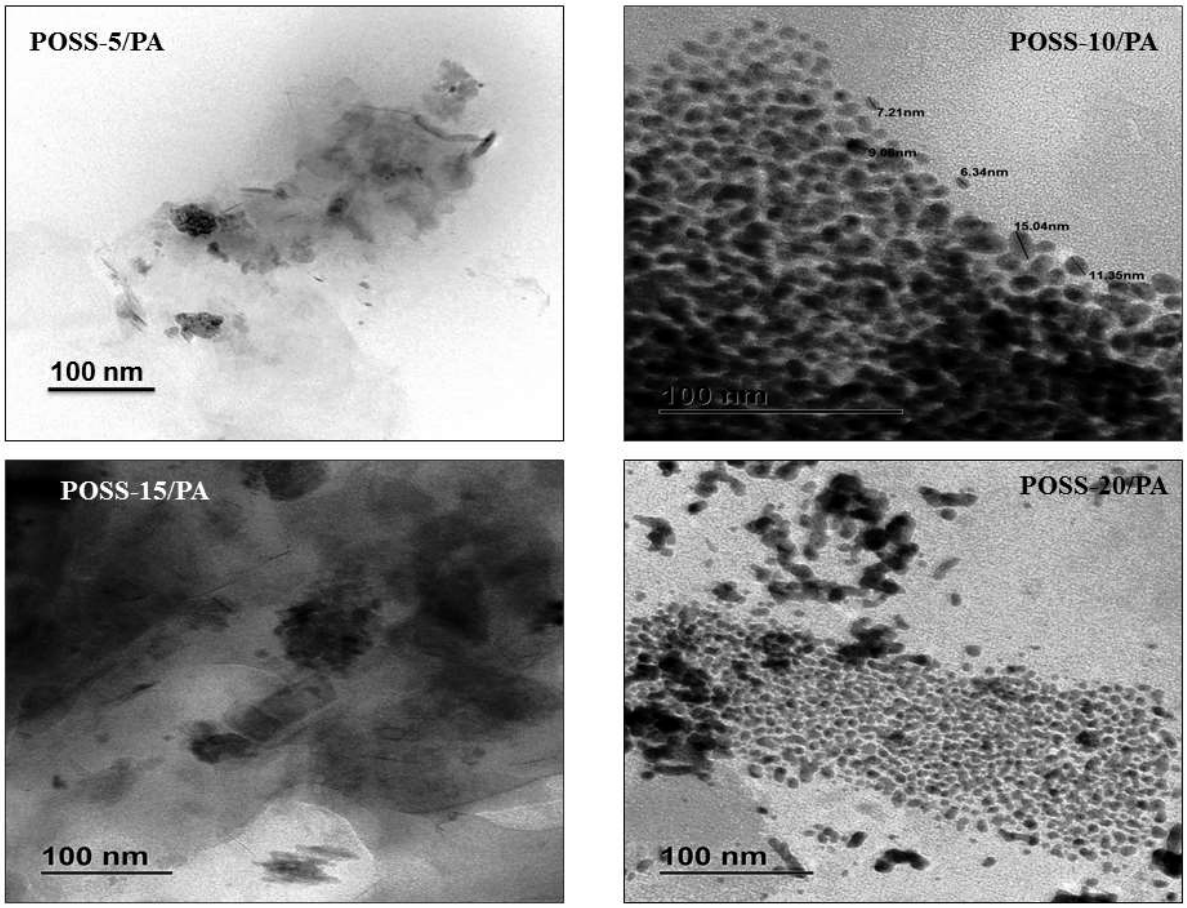

Figure 4: Transmission electron microphotographs of different loadings of POSS on POSS/PA bio-nanocomposite membranes at 100 nm. The well dispersion POSS on polyamide membrane proved the compatibility nature of POSS with polyamide.

Clearly, the hydrogen bonding interactions overcome the attraction force of the POSS and hence, promote uniform dispersion of the POSS in the nanocomposite membranes. Similar type of dispersions were observed by Ayandele et al [11] and Roy et al.[48] This increased the compatibility between the two components, leading to a nanosized dispersion of some POSS molecules. The TEM images showed slight increase in the aggregation pattern on increasing the POSS content from 5% to 20%.

3.3.2. Scanning electron microscopy and EDX

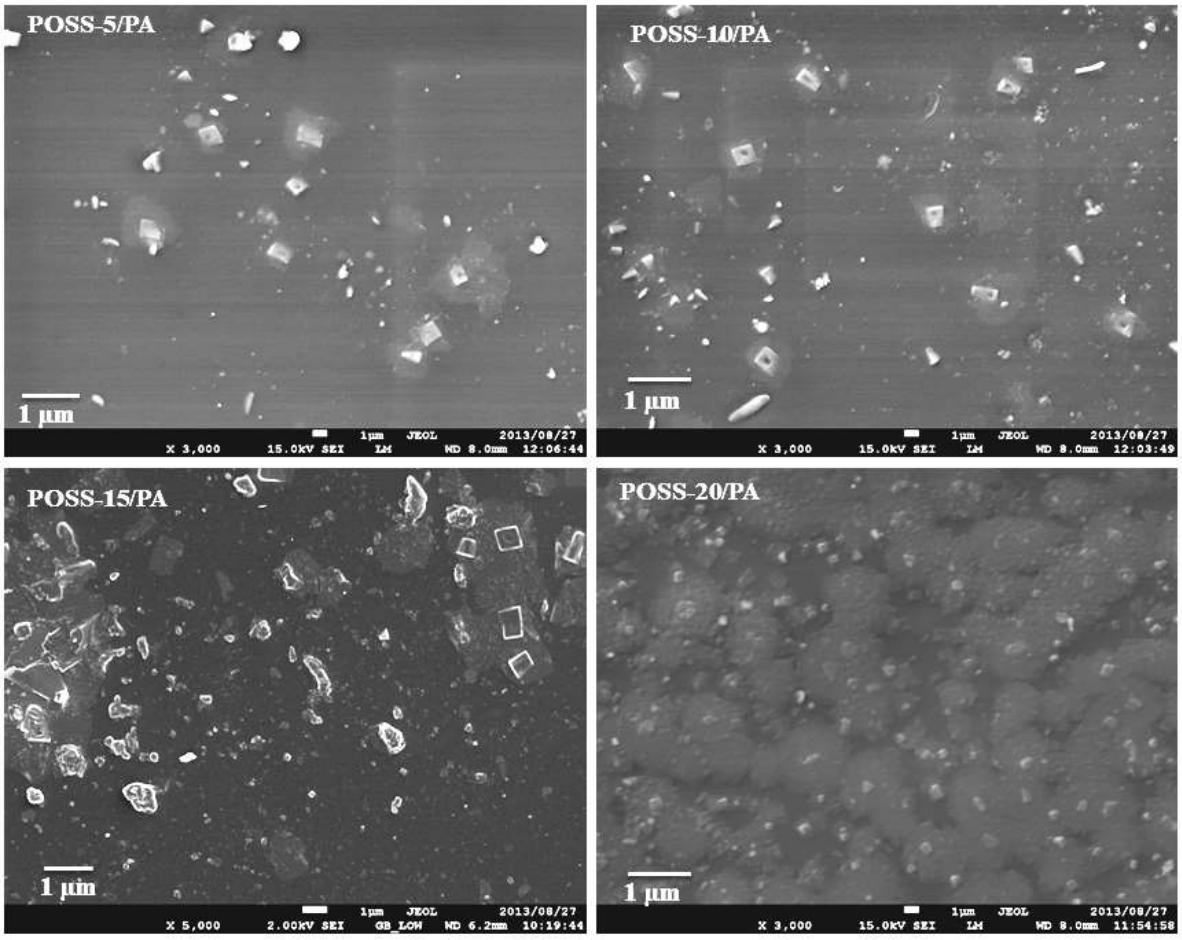

Figure 5: SEM images (taken at 1 µm) of POSS/PA membranes showed homogenous dispersion of POSS. Although, the image of POSS-20/PA shows decrease in homogeneity in the dispersion POSS.

The bio-nanocomposite membranes prepared with different loadings of POSS were analysed by scanning electron microscope and the images obtained are given in Fig. 5. All the images invariably contain white points, which indicate the enriched POSS regions in the membranes and very less discernible phase separation is found in the SEM micrograph of the bio-nanocomposite membrane containing 5 wt.% POSS, which suggests that POSS nanoparticles were dispersed homogeneously throughout the matrix at very low concentration. Dense and homogenous morphologies were observed in the SEM images of all bio-nanocomposite membranes and no bulky agglomerate was observed, even with 20 wt.% of POSS in the membrane. This is mainly due to the intermolecular interactions between the

polymer matrix and the POSS nanoparticles.[26, 48] Although, a close examination of these images revealed a gradual decrease in the homogenous dispersion of POSS when the POSS content in the membranes increased.[27, 50]

Fig. 6 shows a typical surface morphology SEM–EDX image for the POSS 5 wt.% and 15 wt.% nanocomposite membranes. These membranes appear to be relatively uniform and thus, indicating that the physical attachment of POSS to the polymer helps to reduce POSS aggregation on the membrane surface and results in good dispersion of the nanoparticles throughout the membrane at lower amount of POSS. Similar results have also been observed by Worthley et al.[28] Lighter regions, ranging in size from a few nanometers up to a few microns in diameter (Fig. 4), contained a peak at 1.7 keV, corresponding to silicon. Increased silicon counts (lighter regions) concentrations were observed, indicating that high POSS nanoparticles were presented within the membranes.

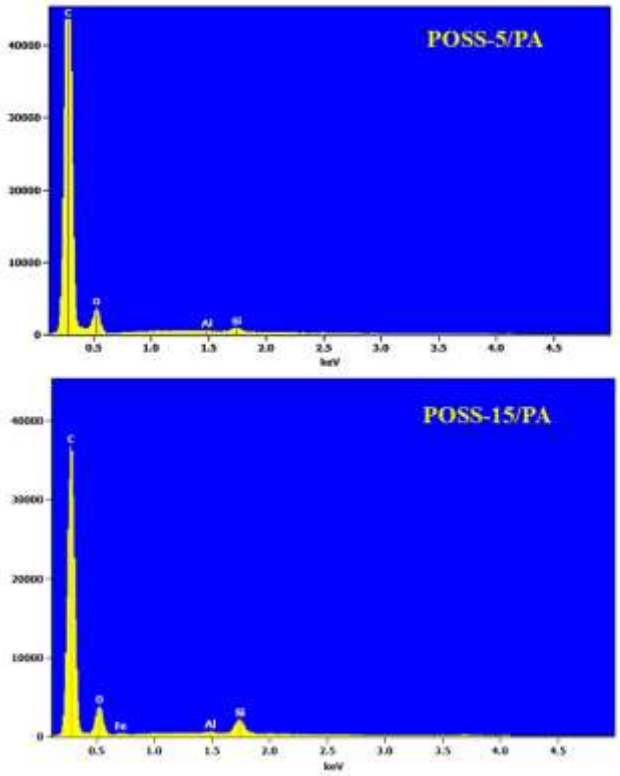

Element Line	Weight %	Weight % Error	Atom %	Atom % Error
C K	90.73	± 0.23	93.01	± 0.24
O K	8.84	± 0.19	6.80	± 0.15
Al K	0.04	± 0.01	0.02	± 0.00
Si K	0.39	± 0.01	0.17	± 0.00
Si L	---	---	---	---
Total	100.00		100.00	

Element Line	Weight %	Weight % Error	Atom %	Atom % Error
C K	82.11	± 0.23	87.50	± 0.25
O K	14.04	± 0.23	11.23	± 0.19
Al K	0.13	± 0.02	0.06	± 0.01
Si K	3.53	± 0.03	0.90	± 0.09
Si L	---	---	---	---
Fe K	0.18	± 0.02	0.20	± 0.01
Fe L	---	---	---	---
Total	100.00		100.00	

Figure 6: SEM-EDX profile of POSS-5/PA and POSS-15/PA bio-nanocomposite membranes present the elemental composition in them.

These observations are further supported by the cross-sectional images of the membranes. Fig. 7 shows the SEM cross-sectional images of the nanocomposite membranes containing 5, 10, 15 and 20 wt.% of POSS. These images exhibit no cracks, voids and defects at the polymer-particle interface, which indicate the excellent dispersion of POSS particles, as observed in the surface of membranes.[18, 19] As mentioned earlier, this is attributed to the formation of effective hydrogen bonds between the hydroxyl groups of POSS and the amide groups of polymer. It is clearly evident from Fig. 5 that the SEM image of membrane with 0 wt % POSS contains a smooth surface (not shown here), whereas a disruption in the smoothness, due to the addition of POSS, is observed in the SEM images of 10 and 20 wt.% POSS incorporated membranes.[13, 27] Generally, this disruption improves the gas-transport ability of the membranes.[15, 23]

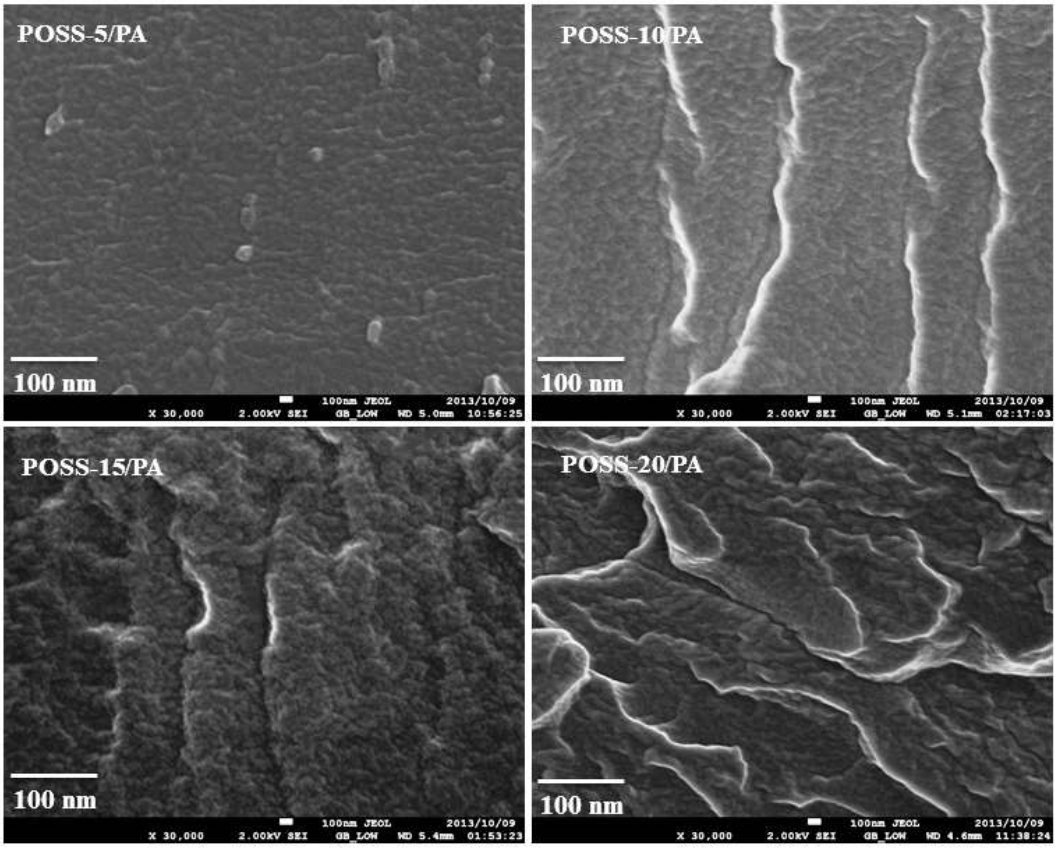

Figure 7: Cross section SEM images (taken at 100 nm) of POSS/PA bio-nanocomposite membranes. The inner surface of the membrane displays no cracks, voids and defects at all concentrations of POSS in POSS/PA membranes.

3.3.3.Atomic force microscopy

The bio-nanocomposite membranes were also analyzed by atomic force microscope (AFM) in order to explore the surface morphology in three dimensions and the height of the images. The AFM height (topographic) and the 3D images were simultaneously obtained under tapping conditions on the surface of bio-nanocomposites and are shown in Fig. 8. The dark and light regions that appeared in the AFM height and 3D images denote the highest and lowest points of the surface of POSS-polymer matrix.[14] Moreover, the maximum vertical distance between the highest and lowest point for 5 wt.% POSS is 35 nm, while that of the 20 wt.% POSS incorporated nanocomposite sample is found to be 82 nm. The roughness parameters are listed in Table 1 where R_{max}, R_q and R_a represent the maximum height, route mean squared variation of height and the average deviation of height, respectively. It is clear from the Table 1 that the incorporation of POSS into the polymer matrix increases the surface roughness of the materials. Similar results have been observed by Rahman et al. [14] For example, the calculated surface roughness of the membranes with 20 is higher than that of membranes with lower wt.% POSS. This may due to the reorganization of the polymer chains in order to accommodate the POSS nanoparticles in the polymer matrix.[15, 51] The AFM 3D images (5 μm x 5μm) exhibit high protuberant and clearly visible flakes with a thickness of ~100 nm. The surface microstructure of POSS incorporated membranes was fluctuant and some regions were obviously higher than others (Fig. 8). It is evident from the 3D images that no clusters or agglomerates appeared on the surface of the nanocomposite membrane, even at high level of loading with POSS. This shows the compatibility of the nanoparticles with the polymer matrix.

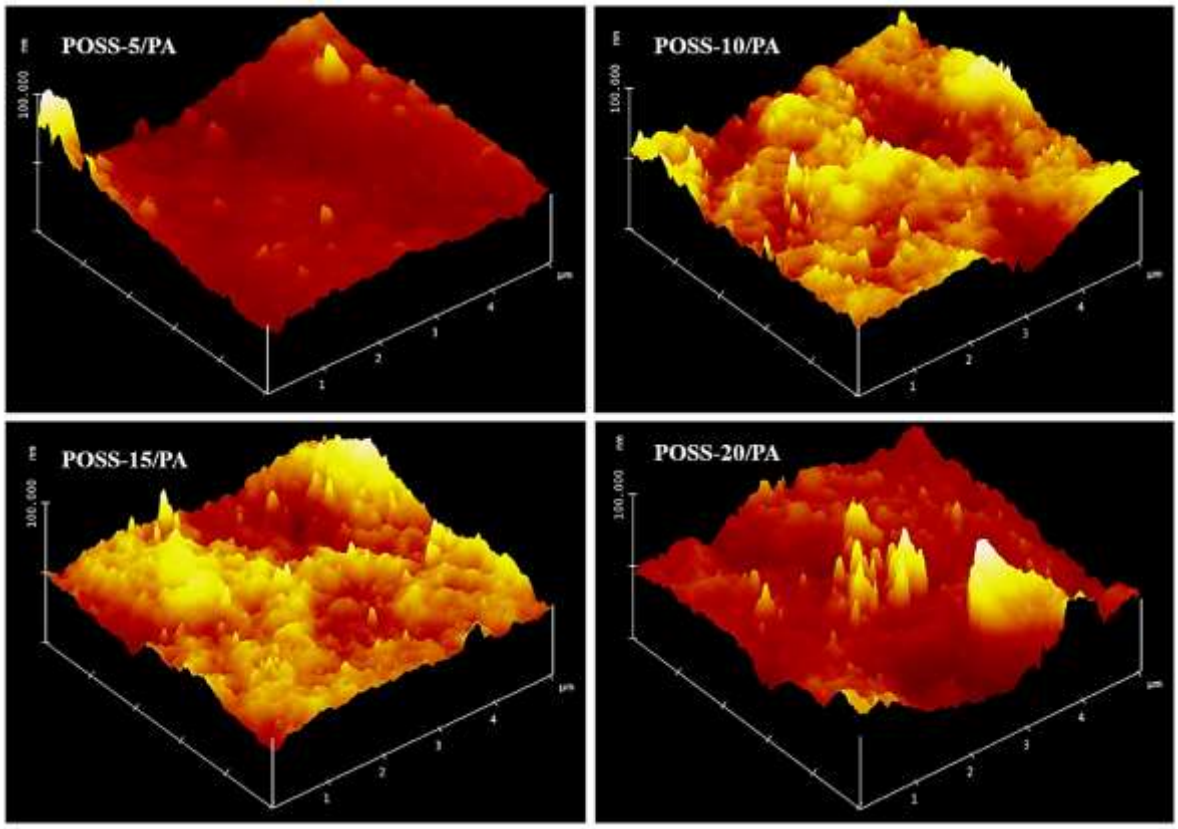

Figure 8: The AFM 3D images (5 μm x 5μm) exhibit high protuberant and clearly visible flakes with a thickness of ~100 nm. Atomic force microscopy (topographic image) presents the change in the surface roughness of POSS/PA membranes by changing the POSS content (from 5% to 20 %). The dim and bright regions denote the highest and lowest points of the surface of POSS/PA bio-nanocomposite.

3.4.Relationship between surface topography and gas separation properties

The three successive steps, namely: sorption of the penetrant at the feed side of the membrane, diffusion of the penetrant through the membrane and desorption at the permeate side, are believed to involve in the gas transport process through the dense polymeric membranes.[2] Adsorption, the first step, needs more available adsorption sites on the membrane surface, which largely depends on the roughness of the surface of the membrane.[14] For example, roughness provides more available adsorption sites than completely smooth surface of membrane. At the same time, roughness does not favor diffusion, the second step. In the present study, the incorporation of POSS, which creates

roughness on the surface, is helpful for adsorption whereas it restricts diffusion. Similar results were obtained by Rahman et al. [14] From Table 1, it is clear that the incorporation of 20 wt.% POSS seemed to have increased the surface roughness of the polymer matrix. Meanwhile, the decrease of gas permeability of the membrane was also significantly higher in case of POSS-20/PA than POSS-0/PA.

As expected, the incorporation of POSS into the matrix, increased density, roughness and selectivity and decreased the free volume and permeability of the membrane.[17]

3.5.Surface free energy of POSS/PA bio-nanocomposite membrane

The contact angle of probe liquids and surface energy of polar/dispersion components of the nanocomposite membranes were calculated and the results are given in Table 2. Both the neat PA and POSS incorporated PA membrane showed water contact angles greater than 80^{o}. In all cases, increase in POSS content showed an increase in the contact angle of water. The increase in the contact angle of water may be due to the highly hydrophobic nature of POSS phases, which spread on the surface of hybrid membranes and proves that an increase in POSS content also increased the hydrophobicity of the membrane surfaces. Similar observation was reported by Gnanasekaran et al.[15] Madhavan and Reddy.[16]

Table 2: Contact angle and surface free energy of POSS/PA bio-nanocomposite membranes

Sample	${}^{\theta}H_2O$	${}^{\theta}C_{16}H_{34}$	γ_s^d (mNm^{-1})	γ_s^p (mNm^{-1})	γ_{sv} (mNm^{-1})
POSS-0/PA	81.33	50.66	18.35	26.55	44.90
POSS-5/PA	83.66	53.66	17.43	24.58	42.01
POSS-10/PA	85.33	54.33	17.23	23.00	40.23
POSS-15/PA	86.33	55.00	17.02	22.13	39.15
POSS-20/PA	87.33	56.66	16.50	21.40	37.90

As was observed in the AFM images, the distributions of POSS in PA chain showed rough surfaces. This in turn, with the POSS-0/PA membrane, the polar amide group spread

over the surface of membranes and thus leads to an increase in the interaction parameter of water with polar amide linkages of the nanocomposite membranes. But, the trend is quite different in the case of POSS incorporated nanocomposite membranes, due to highly hydrophobic nature of the granular-type POSS aggregates on the surface of the hybrid membranes. On the other hand, contact angles for hexadecane increased with an increase in the POSS concentration. From the Table 2, it was found that the surface energies (γ_{sv}) of the membranes were decreased [from 44.9 (POSS-0/PA) to 37.9 mNm^{-1} (POSS-20/PA)] by the increase in POSS content. The POSS-0/PA membrane only shows higher surface energies revealing the fact that POSS incorporated hybrid membrane has rigid polar amide groups on the rough surfaces. It was found that a decrease in the surface energy resulted from an increase in the POSS content. This was mainly attributed to the polar component because of the drastic decrease in γ_S^p, from 26.55 mNm^{-1} (POSS-0/PA) to 21.40 mNm^{-1} (POSS-20/PA).

3.6.Effect of POSS on fractional free volume and density of bio-nanocomposite membranes

FFV is the ratio of the free volume to the observed volume and it is used to characterize the efficiency of chain packing in the polymeric membranes. FFV largely depends on the amount of free volume available in the polymeric matrix.[5, 44] The formation of free volume, on the hand, depends on the fillers dispersed in the membrane matrix.[5, 20, 52] In the present study, effective hydrogen bonding between the bulky POSS and the polymer chains resulted in the conformational reorientations of polymer chains, which leads to the close packing of the chains. As a result, free volume decreases, whereas the density of membrane matrix increases. This is clearly evident from Table 1, where a steady decrease in the size of the free volume and increases in densities manifested following the incorporation of various wt.% of POSS in to the polymer matrix. For example, FFV and density values calculated for the membrane with high POSS content are 0.202 and 1.34, respectively, whereas these values for

the neat membrane were found to be 0.254 and 1.07, respectively. Similar observations were also made by Madhavan and Reddy [16] and Zhang et al. [20] These observations emphasize the influence of POSS on the FFV and density, of membranes with POSS inclusion.

3.7.Effect of POSS on permeability of bio-nanocomposite membranes

The size, shape and the connectivity of the dispersed POSS molecules in the polymeric membranes are highly influence the permeability coefficient. These parameters can change the chain mobility and chain packing of polymer chains and determine the formation (and size) of the free volume and the magnitude of the density of such membranes.[15] FFV and density are the important factors that are related, directly, to the permeability of the membranes. Permeability of the bio-nanocomposite membranes evaluated under different pressures (1–4 bar) at 30 ºC is listed in Table 3. Table 3 shows a drastic decrease in the permeability of gases, N_2, O_2 and CO_2, following the increase of POSS content. As mentioned earlier, FFV decreased when increasing the POSS content. This caused disruption of polymer chain packing and resulted in a decrease in the free volume. Similar decrease in the permeability (with increase in POSS concentration) was observed in POSS incorporated nanocomposite membranes (Maxwell's effect).[15, 16]

Therefore, the observed permeability coefficients satisfy the correlations of permeability with FFV and density. These observations follow a regular trend and highly consistent with the observations reported on similar type of membrane.[21] This, once again, indicated the good compatibility of POSS with polyamide membranes, through hydrogen bonding.[22] When compared to the N_2 and O_2, the permeability of CO_2 was found to be very high. This is attributed to its kinetic parameter which is smaller than the others.[5] Higher interaction of CO_2 with these membranes, leading to high permeability coefficient is attributed to the presence of amide groups. Consequently, the amide, hydroxyls and Si-O-Si groups engaging in H-bonds

were energetically favourable. This confirms that H-bonding networks are a hindrance for gas transport property.[22]

Based on the above observations, it is worthy to predict that there is high compatibility of POSS with polyamide, which significantly alters the permeation of the diffusing gas molecules. The dispersion of bulky POSS phase in the membrane and H-bonds, acts as a blocking agent that produces high resistance route for diffusion molecules.[14]

3.8.Pressure dependency of permeability of bio-nanocomposite membranes

The gas permeability studies were carried out for all POSS/PA bio-nanocomposites membranes as a function of pressure difference and the results obtained are listed in Table 3. With an increase in the penetrant pressure, drastic decreases in the permeabilities of N_2 and O_2 gases were observed. This may be explained as the compression created in the polymer matrix by the presence of POSS, which reduces the free volume for the gas transport.[49] Furthermore, the adsorption of lighter gas on the membrane surface is likely to decrease on increasing the penetrant's pressure. In contrast, the permeability of CO_2, on the other hand, increases with increase in pressure. This is because of the more condensable nature, high adsorption and diffusion of CO_2 gas than the N_2 and O_2 gases. It was however, observed that at high POSS content, the increasing order of CO_2 permeability was slightly reduced with pressure, due to the restriction of interaction in the CO_2 with membrane matrix, caused by the presence of POSS aggregates.[23]

3.9.Selectivity of bio-nanocomposite membranes

Table 4 shows the results of permselectivity studies of bio-nanocomposite membranes with different loadings of POSS and penetrant's pressure. For example, for neat polyamide membrane, the selectivity obtained at 1 bar was 2.03 for $P(O_2)/P(N_2)$ and 10.37for

$P(O_2)/P(N_2)$,and at 4 bar was 2.14 for $P(O_2)/P(N_2)$ and 11.20 for $P(CO_2)/P(N_2)$. A steady increase in the permselectivity was observed on increasing the penetrant's pressure as well as POSS content of the membranes. The same membrane with 20 wt% of POSS was found to have a permselectivity of 2.60 for $P(O_2)/P(N_2)$ and 14.34 for $P(CO_2)/P(N_2)$. This observation shows that an increase in POSS content of the membrane enhances the selectivity performance of the membrane. This is due to the incorporated POSS molecules that are physically embedded within the polymeric network, which is supported by the FT-IR (Fig. 1) and ^{29}Si NMR data (Fig.2).

The O_2/N_2 gas pair selectivities increased slightly with an increase in POSS content as well as with pressure. This is mainly due to the high interactions between O_2 gas and the polar groups (amide) of polymers, silicon and oxygen atoms of POSS, which lead to higher solubility of oxygen gas in the membranes.[22] Likewise, the selectivities of CO_2/N_2 gas pair increased from 11.20 to 14.34 with an increase in POSS content and pressure. This shows that selectivity parameter was controlled by the diffusion of gas molecule through the amide polar groups and the POSS in the membrane.

4. Conclusions

Cost-effective and environmentally-friendly POSS/PA bio-nanocomposite membranes with no cracks or voids were prepared for gas transport studies. The gas-transport properties, such as: permeability and selectivity of the membranes were studied by constant volume/variable pressure method. This study clearly showed that the concentrations of POSS in the bio-nanocomposite membranes played a crucial role in the some physical and gas transport property of the membranes. The POSS/PA bio-nanocomposite shows the good gas transport property because of increasing POSS content, increased the T_g, surface roughness and density of the membranes, on one hand and on the other hand, decreased the FFV and

surface free energy of the membranes. POSS-20/PA membrane was found to be the best membrane for gas transport property among the series. These promising findings and the environmentally-friendly nature of these materials will, no doubt, advance the search for suitable applications of these bio-nanocomposite membranes in the food packaging and the petrochemical industries.

Acknowledgements

Financial support for this research from the Institutional Research Development Programme (IRDP) and the South Africa/Mozambique Collaboration Programme of the National Research Foundation (NRF) is gratefully acknowledged. Dhorali Gnanasekaran acknowledges the support via a Vice-Chancellor postdoctoral fellowship from the University of Pretoria.

References

1 P. Pandey, R.S.Chauhan, *Prog. Polym. Sci.* 2001, **26**, 853-893.

2 E.R. Hensema, *Adv. Mater.* 1994, **6**, 269-279.

3 Y. Yampolskii,*Macromolecules* 2012, **45**, 3298-3311.

4 H.A. Mannan, H.Mukhtar, T. Murugesan, R. Nasir, D.F. Mohshim, A. Mushtaq, *Chem. Eng. Technol.* 2013, **36**,1838-1846.

5 G. Maier,*Angew. Chem. Int. Ed.* 1998, **37**,2961-2974.

6 W.J. Koros, G.K. Fleming, *J. Membr. Sci.* 1993, **83**, 1-80.

7 P. Bernardo, E. Drioli, *Petrol. Chem.* 2010, **50**, 271-282.

8 Z.S. Yin, G.L. Shen, *Xiandai Huagong/Modern Chemical Industry* 2012, **32**, 25-28.

9 H. Cong, M. Radosz, B.F. Towler, Y. Shen, *Sep. Purif. Technol.* 2007, **55**, 281-291.

10 P. Bernardo, E. Drioli, G. Golemme, *Ind. Eng. Chem. Res.* 2009, **48**, 4638–4663.

11 E. Ayandele, B.Sarkar, P. Alexandridis, *Nanomaterials* 2012, **2**, 445-475.

12 R.H.B. Bouma, A.Checchetti, G. Chidichimo, E. Drioli, *J. Membr. Sci.* 1997, **128**, 141-149.

13 Y. Li, T.-S.Chung,*Int. J. Hydrog. Energy* 2010, **35**, 10560-10568.

14 M.M. Rahman, V. Filiz, S. Shishatskiy, C. Abetz, S. Neumann, S. Bolmer, M.M. Khan, V. Abetz, *J. Membr. Sci.* 2013, **437**, 286-297.

15 D. Gnanasekaran, P. Ajit Walter, A. Asha Parveen, B.S.R. Reddy, *Sep. Purif. Technol.* 2013, **111**, 108-118.

16 K. Madhavan, B.S.R.Reddy, *J. Membr. Sci.* 2009, **342**, 291-299.

17 K. Madhavan, D.Gnanasekaran, B.S.R. Reddy,*J. Polym. Res.*2011, **18**, 1851-1861.

18 N.L. Le, Y.P. Tang, T-S. Chung, *J. Membr. Sci.* 2013, **447**, 163-176.

19 N.L. Le, Y. Wang, T-S. Chung, *J. Membr. Sci.* 2011, **379**,174-183.

20 H. Zhang, S. Wang, S.G. Weber, *J. Membr. Sci.* 2013, **443**, 115-123.

21 W. Yave, A. Car, K.V. Peinemann, *J. Membr. Sci.*2010, **350**, 124-129.

22 S. Neyertz, P. Gopalan, P. Brachet, A. Kristiansen, F. Mannle, D. Brown,*Soft Mater.* 2014, **12**, 113-123.

23 D. Gnanasekaran, B.S.R.Reddy, *Clean Technol.Environ. Policy* 2013, **15**, 383-389.

24 K.S. Jang, H.J. Kim, J.R. Johnson, W.G. Kim, W.J. Koros, C.W. Jones, S. Nair, *Chem. Mater.*2011, **23**, 3025-3028.

25 S.H. Phillips, T.S.Haddad, S.J. Tomczak, *Curr. Opin. Solid State Mater. Sci.* 2004, **8**, 21-29.

26 A. Luo, X. Jiang, H. Lin, J. Yin, *J. Mater. Chem.* 2011, **21**,12753-12760.

27 G. Lligadas, J.C. Ronda, M. Galia, V. Cadiz,*Biomacromolecules* 2006, **7**, 3521-3526.

28 C.H. Worthley, K.T. Constantopoulos, M. Ginic-Markovic, E. Markovic, S. Clarke, *J. Membr. Sci.* 2013, **431**, 62-71.

29 J. Wu, P.T.Mather, *Polym. Rev.* 2009, **49**, 25-63.

30 S-W. Kuo, F.-C. Chang, *Prog. Polym. Sci.* 2011, **36**, 1649-1696.

31 D.B. Cordes, P.D.Lickiss, F. Rataboul, *Chem. Rev.* 2010, **110**, 2081–2173.

32 W. Zhang, A.H.E. Muller, *Prog. Polym. Sci.* 2013, **38**, 1121-1162.

33 D. Gnanasekaran, K.Madhavan, B.S.R. Reddy, *J. Sci. Ind. Res.* 2009, **68**, 437-464.

34 R.Y. Kannan, H.J. Salacinski, M. Odlyha, P.E. Butler, A.M. Seifalian,*Biomaterials* 2006, **27**, 1971-1979.

35 T.C. Merkel, B.D.Freeman, R.J. Spontak, Z. He, I. Pinnau, P. Meakin, A.J. Hill,*Science* 2002,**296,**519-522.

36 L. Montero de Espinosa, M.A.R. Meier, *Eur. Polym. J.* 2011,**47**, 837-852.

37 M.A.R. Meier, J.O. Metzger, U.S. Schubert, *Chem. Soc. Rev.* 2007,**36**, 1788.

38 R. Matadi, E. Hablot, K. Wang, N. Bahlouli, S. Ahzi, L. Averous, *Compos. Sci. Technol.*2011, **7**, 674-682.

39 E. Hablot, B. Donnio, M. Bouquey, L. Avérous *Polymer* 2010, **51**, 5895-5902.

40 a) Q. Cheng, L. Jiang, Z. Tang, *Acc. Chem. Res.* 2014, **47**, 1256-1266. b) J. Wang, L. Lin, Q. Cheng, L. Jiang, *Angew. Chem., Int. Ed.* 2012, **51**, 4676-4680. c) J. Wang, Q. Cheng, L. Lin, L. Jiang, *ACS Nano* 2014, **8**, 2739-2745. d) W. Cui, M. Li, J. Liu, B. Wang, C. Zhang, L. Jiang, Q. Cheng, *ACS Nano* 2014, **8**, 9511-9517.

41 A. Macheca, D.Gnanasekaran, W.W. Focke,*Colloid. Polym. Sci.*2014,**292,**669–676.

42 P.P. Pescarmona, M.E. Raimondi, J. Tetteh, B. McKay, T. Maschmeyer,*J. Phys. Chem. A* 2003,**207**, 8885-8892.

43 A.A. Bondi, Physical properties of molecular crystals, in: Liquids and Gases. Wiley, New York, 1968.

44 W.M. Lee, *Polym. Eng. Sci.* 1980, **20**, 65-69.

45 D.W. Van Krevelen, P.J. Hoftyzer, Properties of Polymers. Their Estimation and Correlation with Chemical Structure,2nd ed.Elsevier, New York, 1976.

46 C. Wan, F. Zhao, X. Bao, B. Kandasubramanian, M. Duggan, *J. Polym. Sci: Part B: Polym. Phys.* 2009,**47**, 121–129.

47 R. Zhongjie, Z. Rongben, W. Feng, Y. Shouke, *Polym. Chem.* 2011, **2**, 608-613.

48 S. Roy, V. Scionti, S.C. Jana, C. Wesdemiotis, A.M. Pischera, M.P. Espe, *Macromolecules* 2011, **44**, 8064-8079.

49 K. Madhavan, B.S.R.Reddy, *J. Membr. Sci.* 2006, **283**,357–365.

50 C.H. Lu, S.W.Kuo, W.T. Chang, F.C. Chang,*Macromol. Rapid Commun.* 2009, **30**, 2121-2127.

51 R. Misra, B.X. Fu, S.E.Morgan, *J. Polym. Sci. Part B: Polym. Phys.* 2007, **45**, 2441-2455.

52 P. Winberg, K. Desitter, C. Dotremont, S. Mullens, I.F.J. Vankelecom, F.H.J. Maurer, *Macromolecules* 2005, **38**, 3776-3782.

Nomenclature

P	: Permeability coefficient (cm^3(STP).cm/(cm^2.s.cmHg))
J	: Steady state flux (cm^3(STP)/(cm^2.s))
ΔP	: Pressure difference
d	: Thickness of the membranes (cm)
A	: Membrane area (cm^2)
T	: Temperature (°C)
P_a	: Atmospheric pressure (bar)
$\alpha_{A/B}$	: Selectivity of gas A and B
ρ_{film}	: Density of the membrane (g/cm^3)
m_{air}	: Weight of polymer in air(g)
m_{liquid}	: Weight of polymer in liquid (g)
ρ_{liquid}	: Density of the liquid(g/cm^3)
FFV	: Fractional free volume
V	: Total specific volume of the polymer
Vo	: Occupied volume of the polymer
FT-IR	: Fourier Transform Infrared Spectroscopy
TGA	: Thermogravimetric Analysis
SEM	: Scanning Electron Microscopy
TEM	: Transmission Electron Microscopy
EDX	: Energy-dispersive X-ray
CP/MAS NMR	: Cross Polarization Magic Angle Spinning Nuclear Magnetic Resonance
AFM	: Atomic Force Microscopy